

Differential positronium-formation cross sections for Ne, Ar, Kr, and Xe

S. E. Fayer,^{1,*} D. M. Newson,¹ S. J. Brawley,¹ A. Loreti,¹ R. Kadokura,¹ T. J. Babij,² J. Lis,^{1,†} M. Shipman,¹ and G. Laricchia^{1,‡}

¹*UCL Department of Physics and Astronomy, University College London, Gower Street, London, WC1E 6BT, United Kingdom*

²*Research School of Physics and Engineering, Australian National University, Canberra, ACT 2600, Australia*



(Received 20 September 2019; published 19 December 2019)

Experimental determinations of the absolute differential positronium-formation cross sections near 0° for Ne, Ar, Kr, and Xe are presented and compared with theory. The degree of forward collimation, expressed by the ratios of the differential-to-integral positronium-formation cross sections, is also computed and compared with theories and other targets. Trends among targets and structures at low energies emerge when considered as a function of the reduced total energy.

DOI: [10.1103/PhysRevA.100.062709](https://doi.org/10.1103/PhysRevA.100.062709)

I. INTRODUCTION

Positronium (Ps) is a hydrogenlike atom consisting of a positron and its antiparticle, the electron. By studying its properties, formation and scattering (e.g., [1–3], respectively), insights into basic matter-antimatter interactions can be gained (e.g., [4,5] and references therein). The first absolute experimental determinations of the differential Ps formation cross section ($\frac{dQ_{\text{Ps}}}{d\Omega}$) near 0° were obtained for He, Ar, H₂, and CO₂ [2] from measurements of the Ps production efficiency made on the UCL Ps beam line [6]. In the current paper, we present the extension of these studies to Ne, Kr, Xe, and additional data for Ar.

A detailed description of the experimental setup can be found in [7] and [8]. Briefly, a beam of Ps is formed by charge exchange of positrons (e^+) with a gaseous target in a scattering cell. The technique relies on the natural forward collimation of the Ps produced, which is then detected with a channel electron multiplier (CEM or CEMA) in coincidence with one or more γ -ray detectors (CsI and/or NaI). The geometry of the system gives an angular acceptance of 1.2° depending on the positions of various collimators and the CEM or CEMA detector. It has been found that the Ps atoms in the beam are predominately in the ground state [9,10] and the beam has an energy resolution dominated by that of the e^+ beam [for RGS moderators, typically 1 and 2 eV full width at half maximum (FWHM) for Ne and Kr, respectively, in the Kr case with a higher energy tail [3]].

Ps may be formed in singlet (para) or triplet (ortho) states depending on the relative spin orientation of its constituents. These states are characterized by different lifetimes ($\tau_{\text{Ps}} = 142$ ns and 125 ps for 1^3S_1 and 1^1S_0 , respectively) and annihilation modes (dominantly 3- γ and 2- γ , respectively). Only ortho-Ps survives long enough to reach the detection region.

*Present address: Center for Fundamental Physics, Northwestern University, Evanston, Illinois 60208, USA.

†Present address: Department of Physics, University of Colorado, Boulder, Colorado 80309, USA.

‡g.laricchia@ucl.ac.uk

II. METHOD

Following the method of [2], the measured Ps beam production efficiency is expressed as

$$\epsilon_{\text{Ps}}^{\text{m}} = \frac{\epsilon_d^{\text{Ps}} N_{\Delta\Omega}^{\text{Ps}}}{\epsilon_d^+ N_+} = \frac{\epsilon_{\text{Ps}}}{R_d} e^{-t/\tau_{\text{Ps}}}, \quad (1)$$

where $R_d = \epsilon_d^+ / \epsilon_d^{\text{Ps}}$ is the energy-dependent ratio of the detection efficiencies for positrons and Ps [8,11,12], $N_{\Delta\Omega}^{\text{Ps}}$ the number of positronium atoms emitted in a small solid angle $\Delta\Omega$, N_+ the number of incident positrons, ϵ_{Ps} the “true” Ps beam production efficiency and t the flight time of Ps to the detector.

From Eq. (1), Shipman *et al.* [2] obtained the following expression for the differential cross section near zero degrees:

$$\begin{aligned} \frac{dQ_{\text{Ps}}}{d\Omega} &\simeq \frac{4}{3} \frac{\epsilon_{\text{Ps}}^{\text{m}} R_d}{\rho \Delta \ell_+} \\ &\times \left\{ \sum_{\ell_+=0}^L \left[\exp(-\rho \ell_+ Q_{\text{T}}^+) \exp(-\rho(L - \ell_+) Q_{\text{T}}^{\text{Ps}}) \right. \right. \\ &\times \left(\frac{\pi r^2}{(L - \ell_+ + d)^2} \right) \\ &\left. \left. \times \exp\left(-\frac{(L - \ell_+ + d)}{\tau_{\text{Ps}}} \sqrt{\frac{m}{E_{\text{Ps}}}}\right) \right] \right\}^{-1}. \quad (2) \end{aligned}$$

Here ρ is the target number density, ℓ_+ the positron path length through the gas, Q_{T}^+ and Q_{T}^{Ps} are the total cross sections for positron and Ps scattering, respectively, L is the cell length, r the radius of the illuminated area on the detector, d the distance from the exit aperture of the cell to the detector, m the rest mass of a positron (or electron), and E_{Ps} the kinetic energy of Ps. The factor of $4/3$ accounts for spin multiplicity and the summation is in steps of $\Delta\ell_+$ (chosen so that $\rho\Delta\ell_+Q_{\text{T}}^+ \rightarrow 0$) over the length of the cell.

In Eq. (2), values for Q_{T}^+ and Q_{T}^{Ps} available in the literature have been used, interpolating between data points where

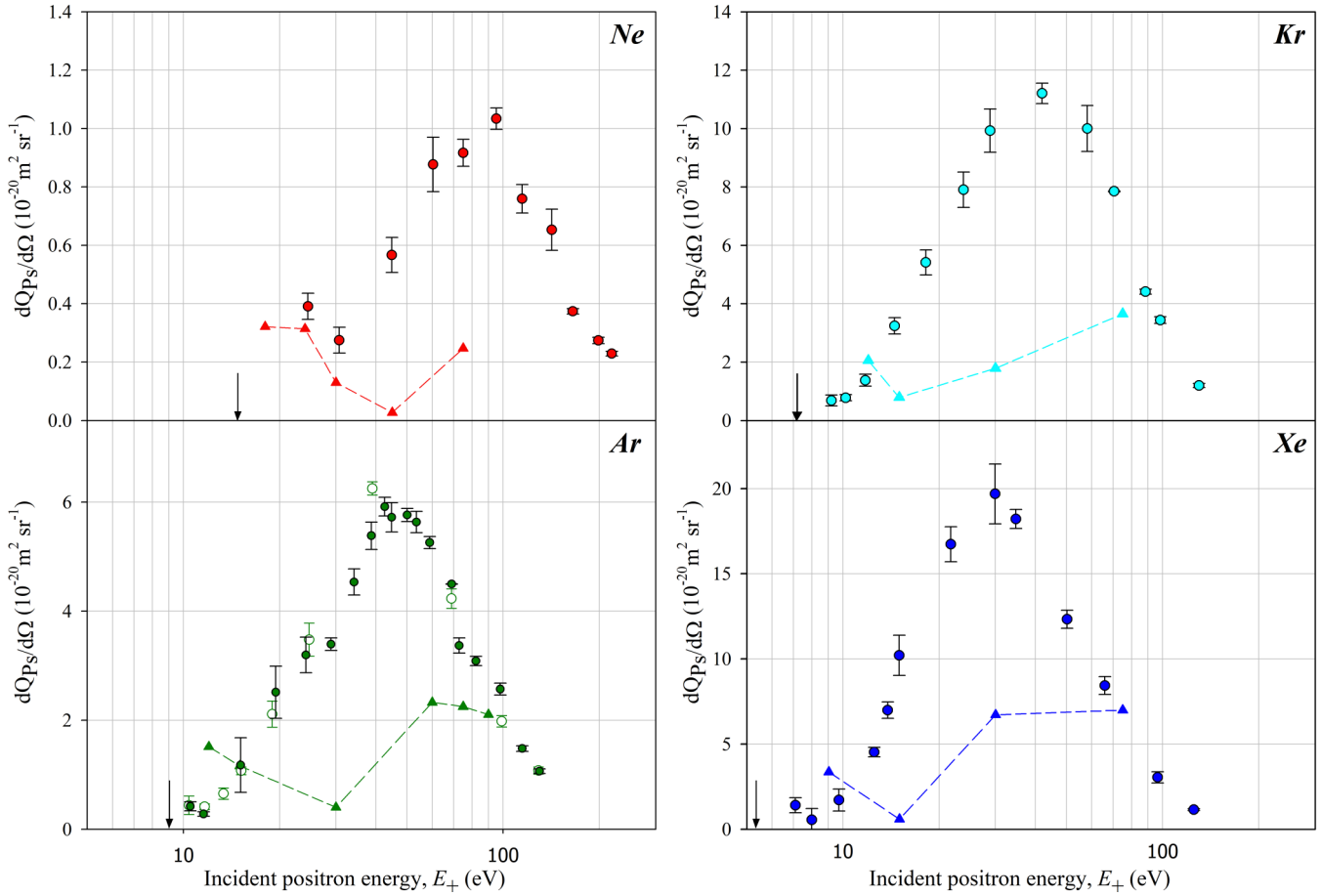


FIG. 1. Current experimental differential cross sections for Ps formation from Ne, Ar, Kr, and Xe (filled circles) compared with determinations from previous production efficiency measurements (hollow circles) [2] and the theoretical results (triangles) of the truncated coupled-static calculation of McAlinden and Walters [13]. The dashed lines are a guide to the eye only. The arrows indicate the Ps formation thresholds.

required. Specifically, data for Q_T^+ in [14–17] and Q_T^{Ps} in [3,9,18,19] for Ne, Ar, Kr, and Xe were used. As expected and verified in our previous work [2], the differential Ps formation cross section was found to be pressure independent within errors for the majority of the data. An apparent pressure dependence may arise if inaccurate values of Q_T^+ and Q_T^{Ps} are used as input to Eq. (2). Here we note that there are only two sets of measurements for Q_T^{Ps} in the case of Ne and Xe [3,18,19] and discrepancies between recent measurements of Q_T^+ for Xe of 5%–15% in the range 7–60 eV [20,21]. Where a pressure dependence (reduced $\chi^2 > 1$) was found, $\frac{dQ_{Ps}}{d\Omega}$ was extracted by varying both Q_T^{Ps} and Q_T^+ systematically as follows. Starting from literature values of Q_T^{Ps} and Q_T^+ , the reduced χ^2 was evaluated for a small increase and decrease in Q_T^{Ps} , Q_T^+ and both. The procedure was continued iteratively until a reduced $\chi^2 \sim 1$ was found. For Xe, which showed the greatest pressure dependence, Q_T^{Ps} and Q_T^+ were changed by a maximum of $\simeq 20\%$ with the majority of changes less than 10%. The resultant change in $\frac{dQ_{Ps}}{d\Omega}$ was a reduction of $\leq 17\%$ for Xe. For Kr, the associated reduction was $\leq 7\%$. At each energy, the final value for $\frac{dQ_{Ps}}{d\Omega}$ corresponds to the arithmetic mean of several sets of measurements of comparable weights. The systematic uncertainty assigned to R_d has been estimated as +8% and from -20% to -30% [11,22]. In the case

of the present results for Ar and Kr, there is an additional systematic uncertainty of 7% arising from the normalization among different sets of runs.

III. RESULTS AND DISCUSSION

The current determinations of $\frac{dQ_{Ps}}{d\Omega}$ with incident positron energy E_+ for Ne, Ar, Kr, and Xe are shown in Fig. 1, the positronium-formation thresholds (E_{th}) for these targets (14.76 eV, 8.96 eV, 7.20 eV, and 5.33 eV, respectively) are indicated in the figure by arrows. Also shown in the figure are previous measurements [2]. The maximum of $\frac{dQ_{Ps}}{d\Omega}$ for Xe is approximately 1.8 times that for Kr, over 3 times that for Ar and about 20 times that for Ne. Included in Fig. 1 are the results of the only available theory for these targets, the truncated coupled-static calculation of McAlinden and Walters [13], the magnitude of which is broadly consistent with experimental data at low and high energies but a factor of 3–5 times lower in the region of the experimental peak. Also of note is the slight initial drop in $\frac{dQ_{Ps}}{d\Omega}$ with increasing energy predicted by the theory for all targets.

The forward collimation of the Ps formed in (e^+ + atom) collisions, expressed by the ratio $\frac{dQ_{Ps}}{d\Omega}/Q_{Ps}$, is shown in Fig. 2. For Ne, Ar, Kr, and Xe, this is computed using experimental

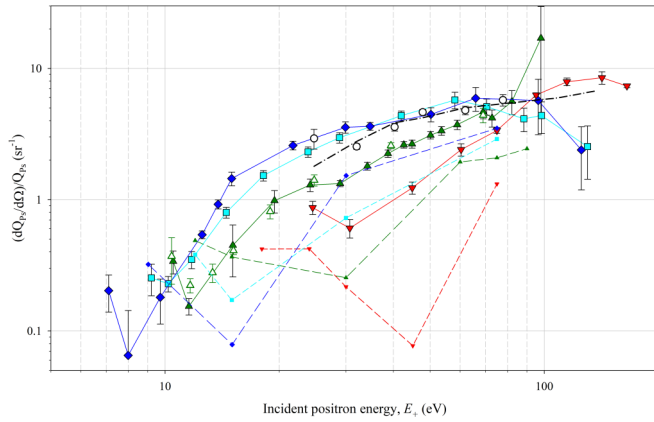


FIG. 2. A comparison of the ratio $\frac{dQ_{Ps}}{d\Omega}/Q_{Ps}$ for the atoms investigated in this (filled) and previous (hollow) work [2]: (circles) He; (down triangles) Ne; (up triangles) Ar; (squares) Kr; and (diamond) Xe. Theories: (dash-dot line) 27-state coupled-pseudostate approach for He [23,24]; truncated coupled static theory [13] for the following: Ne (small down triangles); Ar (small up triangles); Kr (small square); and Xe (small diamond). The dashed lines are a guide to the eye only.

values of Q_{Ps} from [25] and it is compared with those for He and Ar of [2]; at higher energies, the large uncertainties arise mainly from those in Q_{Ps} [25]. Generally, the experimental $\frac{dQ_{Ps}}{d\Omega}/Q_{Ps}$ is similar for all targets, except neon for which the collimation is significantly lower at intermediate energies (perhaps arising from a combination of its low polarizability [26] and of the angular momentum of the captured p electron [27]), approaching those of the other atoms with increasing energy. Also illustrated in Fig. 2 are the results of the truncated coupled static theory of [13,28] for Ne, Ar, Kr, and Xe as well as, in the case of He, of the 27-state coupled-pseudostate approximation of Walters and co-workers [23,24]. While in the case of He, the agreement between theory and experiment is excellent, for the heavier inert atoms, the accord is only qualitative across the targets.

Following the work of [29] in which the lognormal function was found to describe the energy dependence of a variety of inelastic collisions by allowing for the relevant threshold energy, we plot in Fig. 3(a) the values of $\frac{dQ_{Ps}}{d\Omega}$ versus $(\frac{E'}{E_{th}})$, i.e., the total energy ($E' = E_+ - E_{th}$) scaled by the corresponding Ps formation threshold energy. Here we note that, when considered in combination, also the experimental cross sections for Ne, Ar, Kr, and Xe initially appear to decrease with scaled energies before rising again, consistently with theory of Walters and coworkers [13]. The magnitude of the cross sections increases with the target atomic number except for Ne which is lower than for He, once again in qualitative agreement with [13].

Plotting also the forward collimation $\frac{dQ_{Ps}}{d\Omega}/Q_{Ps}$ as a function of $(\frac{E'}{E_{th}})$ in Fig. 3(b), we note that the experimental data for all heavier inert atoms fall broadly on the same curve with a slope similar to that of the corresponding theory of [13,28] as well as of the experimental [2] and theoretical [23,24] data for He. The data for helium at low energies is up to an order of magnitude higher than for the other targets. That He and H₂ [2] provide the highest degree of collimation for atoms and molecules, respectively, might be

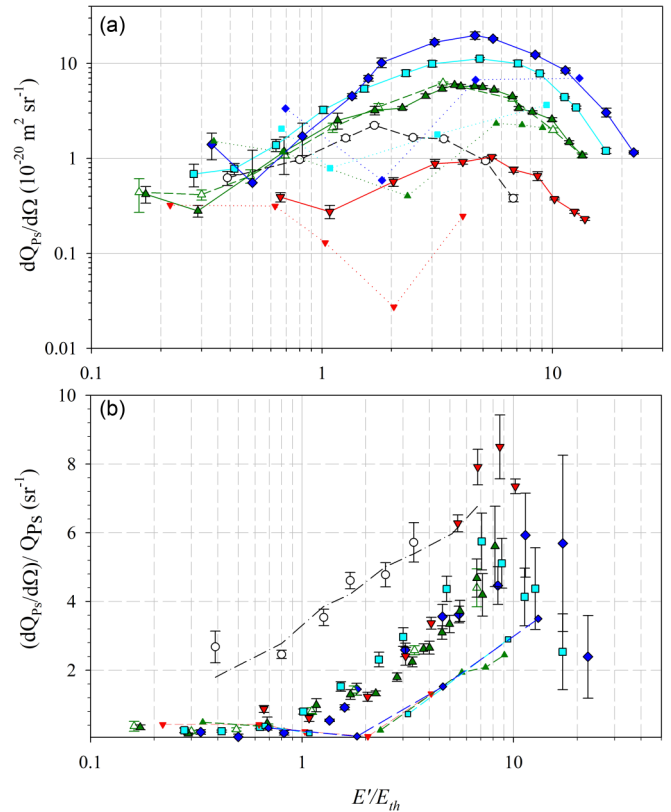


FIG. 3. (a) A comparison of $\frac{dQ_{Ps}}{d\Omega}$ versus the reduced total energy $(\frac{E'}{E_{th}})$ for the atoms investigated in this (filled) and in previous (hollow) work [2]: (circles) He; (down triangles) Ne; (up triangles) Ar; (squares) Kr; and (diamond) Xe. (b) A comparison of the ratio $\frac{dQ_{Ps}}{d\Omega}/Q_{Ps}$ versus the reduced total energy $(\frac{E'}{E_{th}})$ for the atoms investigated in this (filled) and in previous (hollow) work [2]: (circles) He; (down triangles) Ne; (up triangles) Ar; (squares) Kr; and (diamond) Xe. Theories: (dash-dot line) 27-state coupled-pseudostate approach for He [23,24]; the truncated coupled-static theory [13] for Ne (small down triangles); Ar (small up triangles); Kr (small square); and Xe (small diamond). The dashed lines are a guide to the eye only.

linked to their low atomic number (hence low static repulsion) and/or zero angular momentum of the captured electron. The experimental data for the heavier inert atoms suggest minima around $(\frac{E'}{E_{th}}) \approx 0.3-0.5$. The theoretical results for $\frac{dQ_{Ps}}{d\Omega}/Q_{Ps}$ [23,24] also indicate a dip albeit at a somewhat higher energy (≈ 2).

Deep minima in the differential cross sections, at angles greater than 0° , for photo- and electron-impact ionization have been linked to the formation of quantum vortices, an intrinsic property of the velocity fields of complex, time-dependent Schrödinger wave functions, arising when both the real and imaginary parts of the wave function separately vanish [30–32]. These have also been predicted to occur for positron-impact ionization [33]. In the case of positronium formation, minima occurring in the differential cross sections for H at 57° and 51° were discussed by Drachman *et al.* [34] who pointed out that similar features may also occur for He but at smaller angles because of the increased nuclear charge, a conjecture confirmed by the calculations of [35] within a distorted-wave approximation. Whether the

low energy features in Fig. 3 for targets with much greater nuclear charges are related to these phenomena is an open question; however we note that recent elaborate variational calculations for positronium formation in $e^+ + \text{H}$ collisions have established that vortices can indeed occur also for charge exchange [36].

IV. CONCLUSIONS AND OUTLOOK

The absolute $\frac{dQ_{\text{Ps}}}{d\Omega}$ have been measured near 0° for Ne, Ar, Kr, and Xe and compared with theories where possible. The forward collimation of the Ps produced has also been examined and similarities found among $(\frac{dQ_{\text{Ps}}}{d\Omega}/Q_{\text{Ps}})$ when plotted as a function of the reduced total energy $(\frac{E'}{E_{\text{th}}})$. Structures in the form of shallow dips have been noted at low energies and the question raised as to whether they may

be indicative of quantum vortices at larger angles. Further explorations at low energies and over a broader angular range are planned. In this respect, theoretical guidance would be invaluable.

The data supporting this publication are available at UCL Discovery [37].

ACKNOWLEDGMENTS

The Engineering and Physical Sciences Research Council is gratefully acknowledged for supporting this work under Grant No. EP/P009395/1 and for providing S.E.F., M.S., and D.M.N. with research studentships. T.J.B. is grateful for The Robert and Helen Crompton Award. The authors would like to thank John Humberston, Peter Van Reeth, James Walters, and Sandra Ward for valuable discussions.

-
- [1] A. M. Alonso, B. S. Cooper, A. Deller, S. D. Hogan, and D. B. Cassidy, *Phys. Rev. A* **93**, 012506 (2016).
 - [2] M. Shipman, S. Armitage, J. Beale, S. J. Brawley, S. E. Fayer, A. J. Garner, D. E. Leslie, P. Van Reeth, and G. Laricchia, *Phys. Rev. Lett.* **115**, 033401 (2015).
 - [3] S. J. Brawley, S. E. Fayer, M. Shipman, and G. Laricchia, *Phys. Rev. Lett.* **115**, 223201 (2015).
 - [4] G. Laricchia and H. R. J. Walters, *Riv. Nuovo Cimento* **35**, 305 (2012).
 - [5] G. Laricchia, S. Armitage, A. Kövér, and D. J. Murtagh, in *Advances in Atomic, Molecular and Optical Physics*, Vol. 56, edited by E. Arimondo, P. R. Berman, and C. C. Lin (Academic Press, Cambridge, 2008), pp. 1–47.
 - [6] M. Shipman, S. J. Brawley, L. Sarkadi, and G. Laricchia, *Eur. Phys. J. D* **68**, 66 (2014).
 - [7] A. Özen, A. J. Garner, and G. Laricchia, *Nucl. Instrum. Methods Phys. Res. Sect. B* **171**, 172 (2000).
 - [8] M. Shipman, S. Brawley, D. Leslie, S. Armitage, and G. Laricchia, *Eur. Phys. J. D* **66**, 96 (2012).
 - [9] A. J. Garner, A. Özen, and G. Laricchia, *Nucl. Instrum. Methods Phys. Res. Sect. B* **143**, 155 (1998).
 - [10] G. Laricchia, S. Armitage, and D. E. Leslie, *Nucl. Instrum. Methods Phys. Res. Sect. B* **221**, 60 (2004).
 - [11] S. Armitage, D. E. Leslie, A. J. Garner, and G. Laricchia, *Phys. Rev. Lett.* **89**, 173402 (2002).
 - [12] M. Shipman, S. J. Brawley, D. M. Newson, T. J. Babij, and G. Laricchia (unpublished).
 - [13] M. T. McAlinden and H. R. J. Walters, *Hyperfine Interact.* **89**, 407 (1994).
 - [14] L. Chiari and A. Zecca, *Eur. Phys. J. D* **68**, 297 (2014).
 - [15] M. S. Dababneh, Y. F. Hsieh, W. E. Kauppila, V. Pol, and T. S. Stein, *Phys. Rev. A* **26**, 1252 (1982).
 - [16] W. E. Kauppila, T. S. Stein, J. H. Smart, M. S. Dababneh, Y. K. Ho, J. P. Downing, and V. Pol, *Phys. Rev. A* **24**, 725 (1981).
 - [17] S. Fayer, A. Loreti, S. L. Andersen, A. Kover, and G. Laricchia, *J. Phys. B: At. Mol. Opt. Phys.* **49**, 075202 (2016).
 - [18] D. M. Newson, S. Brawley, and G. Laricchia (unpublished).
 - [19] S. J. Brawley, S. Armitage, J. E. Beale, D. E. Leslie, A. I. Williams, and G. Laricchia, *Science* **330**, 789 (2010).
 - [20] A. Zecca, L. Chiari, E. Trainotti, D. V. Fursa, I. Bray, A. Sarkar, S. Chattopadhyay, K. Ratnavelu, and M. J. Brunger, *J. Phys. B: At. Mol. Opt. Phys.* **45**, 015203 (2012).
 - [21] J. R. Machacek, *New J. Phys.* **13**, 125004 (2011).
 - [22] S. Armitage, Ph.D. thesis, University College London, 2002.
 - [23] H. R. J. Walters (private communication) (2015).
 - [24] C. P. Campbell, M. T. McAlinden, A. A. Kernoghan, and H. R. J. Walters, *Nucl. Instrum. Methods Phys. Res. Sect. B* **143**, 41 (1998).
 - [25] G. Laricchia, P. Van Reeth, M. Szłuińska, and J. Moxom, *J. Phys. B: At. Mol. Opt. Phys.* **35**, 2525 (2002).
 - [26] D. D. Reid and J. M. Wadehra, *Phys. Rev. A* **50**, 4859 (1994).
 - [27] J. Moxom, G. Laricchia, M. Charlton, A. Kövér, and W. E. Meyerhof, *Phys. Rev. A* **50**, 3129 (1994).
 - [28] M. T. McAlinden and H. R. J. Walters, *Hyperfine Interact.* **73**, 65 (1992).
 - [29] G. Laricchia, P. Van Reeth, S. E. Fayer, S. J. Brawley, R. Kadokura, A. Loreti, and M. Shipman, *Sci. Rep.* **8**, 15056 (2018).
 - [30] J. H. Macek, J. B. Sternberg, S. Y. Ovchinnikov, T.-G. Lee, and D. R. Schultz, *Phys. Rev. Lett.* **102**, 143201 (2009).
 - [31] J. H. Macek, J. B. Sternberg, S. Y. Ovchinnikov, and J. S. Briggs, *Phys. Rev. Lett.* **104**, 033201 (2010).
 - [32] J. M. Ngoko Djiokap, S. X. Hu, L. B. Madsen, N. L. Manakov, A. V. Meremianin, and A. F. Starace, *Phys. Rev. Lett.* **115**, 113004 (2015).
 - [33] F. Navarrete and R. Barrachina, *J. Phys. B: At. Mol. Opt. Phys.* **48**, 055201 (2015).
 - [34] R. J. Drachman, K. Omidvar, and J. H. McGuire, *Phys. Rev. A* **14**, 100 (1976).
 - [35] P. Mandal, S. Guha, and N. C. Sil, *J. Phys. B: At. Mol. Opt. Phys.* **12**, 2913 (1979).
 - [36] A. W. Alrowaily, S. J. Ward, and P. Van Reeth, *J. Phys. B: At. Mol. Opt. Phys.* **52**, 205201 (2019).
 - [37] UCL Discovery, <http://discovery.ucl.ac.uk/id/eprint/>.